c-Maf is indispensable for the microenvironment of definitive erythropoiesis as it forms erythroblastic islands in fetal liver

c-Maf は胎児肝臓での赤芽球島形成を介する赤血球二次造血のための微小環境に必須である。

２０１１

筑波大学大学院博士課程人間総合科学研究科

日　下　部　　学

CONTENTS

1. Introduction · 3

2. Materials and methods · 6

2-1. Mice

2-2. Hematologic analysis of fetal liver cells, embryonic blood and adult blood

2-3. Flow cytometry and Cell cycle analysis

2-4. Histology and TUNEL assay

2-5. Colony-forming unit assay

2-6. Reconstitution of hematopoietic system with fetal liver cells

2-7. Preparation of "Native" erythroblastic islands and "Reconstituted" erythroblastic islands

2-8. Microarray analysis of fetal liver macrophages

2-9. Real time RT-PCR analysis of fetal liver macrophages

2-10. Luciferase reporter assay

2-11. Statistical analysis

3. Results · 12

3-1. Lethal erythropoietic deficiency in *c-Maf*$^{-/-}$ embryo.

3-2. Increased apoptotic cell death in *c-Maf*$^{-/-}$ fetal liver

3-3. Impaired fetal liver erythropoiesis due to a non-cell-autonomous effect of c-Maf-deficiency

3-4. c-Maf-deficient fetal liver cells are capable of reconstituting the hematopoietic system of adult mice

3-5. Absence of c-Maf causes impaired erythroblastic island formation in the fetal liver.

3-6. Identification of target genes of c-Maf in fetal liver macrophages.

4. Discussion · 20

5. Acknowledgements · 24

6. References · 25

7. Tables · 30

8. Figure legends · 32

9. Figures · 39

1. Introduction

Definitive erythropoiesis arises in mouse fetal liver around embryonic day (E) 10 onward and subsequently switches to postnatal bone marrow and spleen, in which enucleated red blood cells emerge.[1] During terminal erythroid differentiation, erythroblasts are associated with a central macrophage, which forms a specialized microenvironment, the so-called erythroblastic islands. In the erythroblastic islands, a central macrophage provides favorable proliferative and survival signals to the surrounding erythroblasts, and it eventually engulfs the extruded nuclei of maturing erythrocytes.[2-6] Inhibition of the interaction between macrophage and erythroblasts usually leads to embryonic anemia accompanied by accelerated apoptosis of erythroid cells. Targeted disruption of either the transcription factor Rb (retinoblastoma) or actin cytoskeleton associated protein palld (palladin) prevented effective erythroblast-macrophage interactions due to differentiation defects in the macrophage. Therefore, mouse embryos homozygous for either mutant gene suffer from severe anemia and succumb in the embryonic period.[7,8] Meanwhile, it has been reported that a series of adhesion molecules are also involved in the process of forming erythroblastic islands. Erythroblast macrophage protein (EMP) is a 33~36 kDa transmembrane protein expressed in both erythroblasts and macrophages, and it mediates the erythroblast-macrophage interaction. Indeed, the targeted deletion of EMP causes lethal anemia in mouse embryos due to the suppressed formation of erythroblastic islands.[9] Furthermore, a previous report demonstrated that the interaction between very late antigen-4 ($\alpha_4\beta_1$ integrin) on erythroblasts and vascular cell adhesion molecule 1 (VCAM-1) on macrophages plays a key role in maintaining the islands.[10] For example,

administration of antibodies raised against either $\alpha_4\beta_1$ integrin or VCAM-1 caused disruption of the island structure and the resultant erythropoietic deficiency[10]. However, the molecular mechanism, in terms of transcriptional regulation of island-affiliated genes in macrophages, remains largely unknown.

The large Maf transcription factor c-Maf is a cellular homolog of v-maf, which was isolated from a chicken musculoaponeurotic fibrosarcoma induced by avian retrovirus AS42 infection.[11] The large Maf transcripton factors, i.e., MafA/L-Maf/SMaf, MafB, c-Maf and NRL, contain an acidic domain that promotes transcriptional regulation and a basic region/leucine zipper domain that mediates dimerization, as well as DNA binding to either Maf recognition elements (MAREs) or the 5′ AT-rich half-MARE.[12-14] Each large Maf protein has been shown to play a distinct role in cellular proliferation and differentiation in both pathological and physiological situations.[11,15-21] In B-lymphoid and T-lymphoid lineages, aberrant expression of c-Maf works as an oncogene, as shown in multiple myeloma and angioimmunoblastic T-cell lymphoma (AITL) patients and in a transgenic mouse model.[22-25] Physiological c-Maf expression is indispensable for the proper regulation of interleukin (IL)-4 and IL-21 gene expression in T-helper cells.[26,27] In macrophages, c-Maf has been reported to regulate IL-10 expression, which is essential for differentiation of regulatory T-cells.[28] In addition, combined deficiency of MafB and c-Maf enables long-term expansion of differentiated, mature macrophages.[29] We recently reported that c-Maf is abundantly expressed in fetal liver macrophages and that it regulates expression of F4/80, which mediates

immune tolerance.[30] However, the physiological consequences of c-Maf deletion on terminal erythroid differentiation in erythroblastic islands have been largely unexplored.

In the present study, we demonstrate that c-Maf-deficient mice exhibit embryonic anemia, which is associated with a failure to form erythroblastic islands. Moreover, we found significantly reduced expression of VCAM-1 in c-Maf-deficient macrophages, which presumably accounts for the deficiency in island formation and subsequent embryonic anemia. Thus, these results suggest that c-Maf is indispensable for definitive erythropoiesis in fetal liver, as it activates VCAM-1 expression in macrophages, and this causes the formation of erythroblastic islands.

2. Material and methods

2-1. Mice

c-Maf deficient mice were originally generated on a 129/Sv background[16] and have been backcrossed onto a C57BL/6J background for more than seven generations. Genotypes were determined by PCR analysis using tail DNA. In staging the embryos, gestational day 0.5 (E0.5) was defined as noon of the day a vaginal plug was found following overnight mating. Mice were maintained in specific pathogen-free conditions in a Laboratory Animal Resource Center. All experiments were performed according to the Guide for the Care and Use of Laboratory Animals at the University of Tsukuba.

2-2. Hematologic analysis of fetal liver cells, embryonic blood and adult blood

Single-cell suspensions prepared from fetal livers were washed by centrifugation at 1,000 rpm for 5 minutes at 4°C and resuspended in 1 ml of 2% fetal bovine serum/phosphate-buffered saline (PBS). The cell number was counted using a hemocytometer. Collection of embryonic peripheral blood was performed as described previously.[31] In brief, the embryo was dried with the tip of a Kimwipe (Kimberly-Clark, Dallas, TX). Blood was collected with a Microcaps micropipette (Drummond Scientific, Broomal, PA) from the carotid arteries of decapitated embryos. Each sample was centrifuged at 12,000 g for 5 minutes for hematocrit measurement on Hematocrit Centrifuge 3220 (Kubota, Tokyo, Japan). Peripheral blood samples from adult mice were obtained from retro-orbital venous plexus using heparin-coated microtubes. Blood counts were determined with an

automated hemocytometer (Nihon Kohden, Tokyo, Japan). Blood smears were prepared using the wedge technique and were stained with May-Grünwald Giemsa, and then photographed with a KEYENCE BIOREVO BZ-9000 microscope (KEYENCE, OSAKA, Japan). Images were processed using Photoshop software (Adobe, San Jose, CA).

2-3. Flow cytometry and Cell cycle analysis

Freshly isolated fetal liver cells were immunostained at 4°C in PBS/2%FBS in the presence of 5% mouse serum to block Fc receptors. Cells were incubated with fluorescein isothiocyanate (FITC)-conjugated anti-mouse CD71 (eBioscience, San Diege, CA) and allophycocyanin (APC)-conjugated anti-mouse TER-119 (eBioscience) antibodies for 30 minutes at 4°C, followed by a 5-minute incubation with phycoerythrin (PE)-conjugated Annexin V (BioVision, Mountain View, CA) at room temperature. To quantify the presence of VCAM-1 on macrophages, FITC-conjugated anti-mouse Mac-1 (CD11b), biotinylated anti-mouse VCAM-1 and APC-conjugated streptavidin antibodies were used for analyses. For cell cycle analysis, single cell suspensions of E12.5 fetal liver cells were suspended in 4 ml ice-cold 70% ethanol with gentle vortexing, incubated at -20°C for 4 hours, and washed with PBS. Cells were then incubated with 0.2mg/ml RNase (Invitrogen) / PBS at 37°C for 60 minutes. Propidium iodide (PI) was added at a final concentration of 50μg/ml. Flow cytometry was carried out on a Becton Dickinson FACS LSR with CELLQuest (Becton Dickinson) software. Data were analyzed using FlowJo (Tree Star Inc., Ashland, OR) analysis software.

2-4. Histology and TUNEL assay

Whole E13.5 embryos were fixed in 10% formalin neutral buffer solution (Wako, Japan) Paraffin-embedded tissue was sectioned, mounted, and stained with hematoxylin and eosin. Fluorescent terminal dUTP nick-end labeling (TUNEL) assays were performed using an *in situ* Apoptosis Detection Kit according to the manufacturer's protocol (TaKaRa, Tokyo, Japan). Images were captured by a digital camera system using a Leica DM RXA2 microscope (Leica Microsystems, Tokyo, Japan).

2-5. Colony-forming unit assay

Colony-forming unit assays were performed in MethoCult GF M3434 (Stem Cell Technologies) for BFU-E and CFU-GEMM, and M3334 for CFU-E following the manufacturers' instructions. CFU-E were scored two days after plating. BFU-E and CFU-GEMM were scored eight days after plating on coded plates for unbiased counts.

2-6. Reconstitution of hematopoietic system with fetal liver cells

The donor cells for hematopoietic reconstitution were prepared from E14.5 fetal livers of *c-Maf*$^{+/+}$ and *c-Maf*$^{-/-}$ (C57BL/6J-Ly5.1) mice. Suspensions of single fetal liver cells were prepared by mechanical disruption, grinding with a syringe insert against a 70 μm nylon cell strainer (BD-Biosciences, San Jose, CA). Fetal liver cells (2×10^6 cells) were injected into the tail vein of 8-

to 10-week-old C57BL/6J-Ly5.2 mice that were previously exposed to X-ray at the doses of 10 Gy.

2-7. Preparation of "Native" erythroblastic islands and "Reconstituted" erythroblastic islands

Native erythroblastic islands were isolated from fetal livers using a previously described protocol.[7] Briefly, E13.5 fetal livers were dissected and dispersed by enzymatic digestion with collagenase S-1 (Nitta Gelatin, Osaka, Japan) and DNase I (Sigma-Aldrich, St. Louis, MO). Digested fetal liver cells were allowed to attach to glass coverslips for 20 minutes at 37°C in 5% CO_2. Attached cells were then flooded with medium and incubated for 4 hours. Adherent macrophages with attached erythroid clusters were obtained by dipping coverslips in RPMI to remove nonadherent cells and were then processed for immunofluorescence analysis. To strip erythroblasts from macrophages, cells were incubated in PBS lacking Ca^{2+} and Mg^{2+} for 10 minutes. The remaining adherent fetal liver cells were allowed to re-spread in RPMI containing 10% FBS for 2 hours before receiving fresh erythroblasts (*c-Maf*$^{+/+}$ or *c-Maf*$^{-/-}$ E14.5 erythroblasts). Finally, the reconstituted clusters were dipped to remove the unbound cells before being processed for double F4/80-Ter119 immunofluorescence using standard procedures. The number of erythroblasts attached to macrophages was determined by counting the total number of cells present in each island visualized using a Leica fluorescence microscope. Four to six embryos were analyzed per combination group. For each combination, at least 20 macrophages per embryo were analyzed.

2-8. Microarray analysis of fetal liver macrophages

Fetal liver cells from E15.5 *c-Maf*$^{+/+}$ and *c-Maf*$^{-/-}$ embryos were incubated with APC-conjugated anti-Mac-1 antibody (eBioscience) and PE-conjugated anti-F4/80 antibody (Serotec). Mac-1^{+}F4/80^{+} cells were sorted by a FACSAria cell sorter (Becton Dickinson) as fetal liver macrophages. Total RNA was extracted from fetal liver macrophages using a QIAGEN RNeasy Mini Kit according to the manufacturer's instructions. The microarray procedure was performed as described in the Affymetrix GeneChip Expression Analysis Manual (Affymetrix). Biotin-labeled cRNA was synthesized from 4 to 6 μg RNA and hybridized to a GeneChip Mouse Genome 430 2.0 Array (Affymetrix). After washing, arrays were stained with streptavidin-phycoethrin and analysed on a scanner. Each array was analyzed using the GeneSpring (Agilent Technologies, Palo Alto, CA) program to calculate the average density for each prove set (Affymetrix). Data normalization and data analyses were performed using GeneSpring. The data have been deposited in the Gene Expression Omnibus database under the accession number GSE23305.

2-9. Real time RT-PCR analysis of fetal liver macrophages

Macrophages were prepared from E13.5 and E14.5 fetal livers of *c-Maf*$^{+/+}$ or *c-Maf*$^{-/-}$ mice. Suspensions of single fetal liver cells were prepared and Mac-1 positive cells were labeled with Mac-1^{+} magnetic beads to separate macrophages by using the MACS^{TM} system (Miltenyi Biotech). Total RNA was extracted from cells using RNeasy Mini Kit (QIAGEN), and first-strand cDNA was synthesized using QuantiTect Rev. Transcription Kit (QIAGEN). The mRNA levels were examined by real time RT-PCR using Thermal Cycler Dice Real Time System Single (TaKaRa Bio) with a

SYBR Green PCR master mix (TaKaRa Bio). Hypoxanthine guanine phosphoribosyl transferase (*Hprt*) was used as an internal control. The following specific primers were used for PCR: VCAM-1-forward; 5'-GGATGAACACTCTTACCTGTGC, VCAM-1-reverse; 5'-GGTCAAAGGGATACACATTAGGG, EMP-forward; 5'- CCACCAGACACACATATCTC, . EMP-reverse; 5'-CTGCACACAGGGCAGTCAGG, Other primers were as reported previously.[30,32,33]

2-10. Luciferase reporter assay

The *VCAM-1* (-0.7 kilobase (kb)) promoter ligated to a luciferase reporter[34] was transiently co-transfected with c-Maf expression plasmids in macrophage cell line RAW264.7 using Fugene 6 (Roche). Twenty-four hours after the transfection, cells were collected and reporter gene assays were carried out using the Dual Luciferase Kit (Promega, Madison,WI). Transfection efficiency was normalized by measuring expression of *Renilla* Luciferase.

2-11. Statistical analysis

Data were represented as mean plus and minus ~~a~~ standard error of the mean (SEM). Statistical significance between any two groups was determined by the 2-tailed Student *t* test. *p* values less than 0.05 were considered significant.

3. Results

3-1. Lethal erythropoietic deficiency in *c-Maf*$^{-/-}$ embryo.

The *c-Maf*$^{-/-}$ mice, as originally generated, exhibited perinatal mortality within a few hours after birth on a 129/Sv background.[16] However, unexpectedly, on a C57BL/6J genetic background, c-Maf-deficiency resulted in embryonic lethality from E15.5 onward, and almost all *c-Maf*$^{-/-}$ embryos died before E18.5 (Table 1). *c-Maf*$^{-/-}$ embryos at E13.5 showed appearance of a pale fetal liver as well as thin yolk sac blood vessels, in which fewer red blood cells were circulating, compared with healthy *c-Maf*$^{+/+}$ control embryos (Figure 1A). As expected, the hematocrit of peripheral blood in the *c-Maf*$^{-/-}$ embryo (E13.5~E15.5) was markedly reduced (E13.5: 13.4±1.8%, E14.5: 14.5±1.0%, E15.5: 16.9±1.0%), compared with the *c-Maf*$^{+/+}$ control (E13.5: 18.7±0.6%, E14.5: 23.1±1.7%, E15.5: 29.6±1.8%; Figure 1B). May-Grünwald Giemsa staining of peripheral blood smears demonstrated a significant reduction of enucleated red blood cells in *c-Maf*$^{-/-}$ embryos (E13.5: 6.68±1.0%, E14.5: 17.2±1.9%, E15.5: 29.8±5.6%; Figure 1C and D), whereas *c-Maf*$^{+/+}$ control embryos retained normal population of enucleated red blood cells (E13.5: 25.5±4.7%, E14.5: 54.1±1.1%, E15.5: 86.9±2.8%; Figure 1C-D). Considering that the enucleated red blood cells are mainly derived from definitive erythropoiesis, these data suggest that c-Maf-deficient embryos suffer from impaired definitive erythropoiesis on the C57BL/6J genetic background.

3-2. Increased apoptotic cell death in *c-Maf*$^{-/-}$ fetal liver

We next examined the cellular viability as well as the cell cycle status of *c-Maf*$^{-/-}$ fetal liver cells,

in the hope of elucidating the molecular and cellular basis of their erythropoietic deficiency. The fetal liver size in *c-Maf*$^{-/-}$ embryos was smaller, thus consistently fewer number of fetal liver cells were harvested from *c-Maf*$^{-/-}$ embryos between E13.5 and E15.5 (E13.5: 3.37±0.5 ×10^6 cells, E14.5: 7.61±1.0 ×10^6 cells, E15.5: 6.54±2.7 ×10^6 cells) than from age-matched *c-Maf*$^{+/+}$ control embryos (E13.5: 6.89±0.4 ×10^6 cells, E14.5: 16.6±2.3 ×10^6 cells, E15.5: 32.5±2.4 ×10^6 cells) (Figure 2A-B). Of note, hematoxylin-eosin (HE) staining of E13.5 *c-Maf*$^{-/-}$ fetal liver sections demonstrated an increased number of pyknotic nuclei compared to the *c-Maf*$^{+/-}$ control embryo (Figure 2C). Consistently, TUNEL-positive apoptotic cells were remarkably increased in E13.5 *c-Maf*$^{-/-}$ fetal liver sections (Figure 2C). Moreover, flow cytometry analysis of PI-stained fetal liver cells demonstrated an increased abundance of a sub-G0/G1 early apoptotic cell fraction in *c-Maf*$^{-/-}$ fetal liver (8.77±2.5%) compared with *c-Maf*$^{+/+}$ control cells (0.67±0.01%; Figure 2D). However, the cellular population of each phase of the cell cycle, i.e., G_0/G_1, S and G_2/M, was not significantly affected (Figure 2D). Overall, these observations suggest that the fetal liver hematopoietic cells from *c-Maf*$^{-/-}$ embryos are prone to undergo apoptotic cell death.

3-3. Impaired fetal liver erythropoiesis due to a non-cell-autonomous effect of c-Maf-deficiency

Given the significant disturbance of erythropoiesis, we next attempted to delineate the maturation status of erythroid lineage cells in *c-Maf*$^{-/-}$ fetal liver. To this end, we examined fetal liver erythropoiesis by flow cytometry using the erythroid markers CD71 and Ter119, which

distinguish various stages of erythroid-cell differentiation. In the early stages of Ter119^{low} erythroid progenitor development, CD71 expression increases toward the stage of erythroid commitment. However, once they differentiate into Ter119^{high} erythroblasts, CD71 expression decreases during terminal erythroblast maturation.[35] Interestingly, in *c-Maf*$^{-/-}$ fetal liver, the percentages of Ter119^{high} differentiating erythroblasts (R3, R4 and R5 in Figure 3A) were reduced, whereas the percentages of cells in early stages of erythroid progenitors (R1 and R2 in Figure 3A) were increased compared with *c-Maf*$^{+/+}$ fetal liver. Similarly decreased numbers of mature erythroid cells (R3, R4 and R5 in Figure 3B) were observed in *c-Maf*$^{-/-}$ fetal liver as compared with *c-Maf*$^{+/+}$ fetal liver. Consistent with this flow cytometry data, morphological observations of cytospined fetal liver erythroid cells demonstrated that the number of later stage erythroblasts (late basophilic, polychromatophilic and orthochromatophilic erythroblasts) was significantly reduced in *c-Maf*$^{-/-}$ embryos as compared with *c-Maf*$^{+/+}$ controls (Figure 3D). These observations prompted us to quantify the apoptotic cell population in each stage of erythroid cells by annexin V staining in combination with Ter119 and CD71 staining.

In good agreement with the preferential decrease of the late erythroblast population (R3, R4 and R5), we observed a highly increased number of annexin V-positive cells in the more mature erythroblasts (R4 and R5) of *c-Maf*$^{-/-}$ fetal liver as compared with the *c-Maf*$^{+/+}$ fetal liver. In contrast, the premature erythroid progenitors (R1, R2 and R3) of *c-Maf*$^{-/-}$ fetal liver cells exhibited a comparable number of annexin V-positive cells with the *c-Maf*$^{+/+}$ control (Figure 3C). To examine the state of globin regulation, the Mac-1 negative cells from E13.5 fetal liver were sorted by

MACS™ and analyzed for mRNA of β-globin genes by real time RT-PCR analysis. Expression profiles showing switching of β-globin genes demonstrated that the definitive globin gene (βmajor-globin) was significantly down-regulated, while the primitive globin genes (βH1-globin and εy-globin) were not significantly suppressed in the *c-Maf*$^{-/-}$ fetal liver erythroid fraction compared with the *c-Maf*$^{+/+}$ control (Figure 4).

To examine the colony formation potential of hematopoietic progenitors in *c-Maf*$^{-/-}$ fetal liver, conventional set of colony-forming unit (CFU) assays were performed. Eventually we found that there was no significant difference in the number of Burst-Forming Unit-Erythroid (BFU-E) or Colony-Forming Unit-Granulocyte, Erythroid, Macrophage, Megakaryocyte (CFU-GEMM) between *c-Maf*$^{+/+}$ and *c-Maf*$^{-/-}$ fetal liver cells (Figure 3E). However, the Colony-Forming Unit-Erythroid (CFU-E) count was increased about two-fold in *c-Maf*$^{-/-}$ fetal liver cells compared with *c-Maf*$^{+/+}$ fetal liver. Moreover, erythroid cells derived from *c-Maf*$^{-/-}$ CFU-Es exhibited a similar morphology and an equivalent number of enucleated red blood cells as those from *c-Maf*$^{+/+}$ control CFU-Es, in cytospin slides stained with May-Grünwald Giemsa (Figure 5A-B). Taken together, these results suggest that *c-Maf*$^{-/-}$ erythroid cells are still capable of differentiating into mature red blood cells, therefore the impaired definitive erythropoiesis in the *c-Maf*$^{-/-}$ embryos is more likely due to a non-cell-autonomous effect of c-Maf-deficiency.

3-4. c-Maf-deficient fetal liver cells are capable of reconstituting the hematopoietic system of adult mice

To determine whether *c-Maf*$^{-/-}$ embryos still retain hematopoietic stem cells, we tested the ability of c-Maf-deficient fetal liver cells to reconstitute the hematopoietic system of lethally irradiated recipient mice. Fetal liver cells collected from E14.5 *c-Maf*$^{+/+}$ or *c-Maf*$^{-/-}$ embryos were injected into lethally irradiated recipient mice. All recipients receiving both *c-Maf*$^{+/+}$ and *c-Maf*$^{-/-}$ fetal liver cells survived and remained healthy for at least 6 months after transplantation. Consistent with the results obtained from CFU assays, the donor-derived leukocyte chimerism in the mice reconstituted with *c-Maf*$^{-/-}$ fetal liver cells was comparable with that of the recipient mice with control fetal liver cells (Figure 6A). Moreover, there were no significant differences in hematocrit or proportion (%) of B220^{+}, CD4^{+}, CD8^{+}, or Mac^{+}/Gr1^{+} cells between the recipients receiving *c-Maf*$^{+/+}$ or *c-Maf*$^{-/-}$ fetal liver cells (Table 2 and Figure 6B).

Next, we tried to examine whether erythroblast differentiation in bone marrow and spleen was perturbed. Each stage of the erythroblasts was prospectively separated by a similar flow cytometry protocol using TER-119 and CD71 antibodies, i.e., TER-119^{+}/CD71^{+} cells consisting of immature erythroblasts, whereas TER-119^{+}/CD71^{-} cells corresponded to mature erythroblasts. The percentages of TER-119^{-}/CD71^{+} cells, TER-119^{+}/CD71^{+} cells and TER-119^{+}/CD71^{-} cells in the recipient bone marrow receiving *c-Maf*$^{-/-}$ fetal liver cells were comparable to those in the recipient with *c-Maf*$^{+/+}$ fetal liver cells (Figure 6C). Similar results were also observed using spleen cells (Figure 6D). Overall, these results indicate that *c-Maf*$^{-/-}$ hematopoietic cells are able to reconstitute the hematopoietic system in lethally irradiated mice, and that they have the ability to produce adequate amounts of erythroid cells.

3-5. Absence of c-Maf causes impaired erythroblastic island formation in the fetal liver.

c-Maf is abundantly expressed in fetal liver macrophages, although it is largely missing from the erythroid cells in fetal liver. Therefore, we initially surmised that c-Maf-deficiency in fetal liver macrophages disturbed the proper formation of erythroblastic islands[4], then subsequently led to embryonic anemia. To address this hypothesis, we tried to examine whether *c-Maf*$^{-/-}$ macrophages failed to form erythroblastic islands. For this purpose, we isolated the erythroblastic island from *c-Maf*$^{+/+}$ and *c-Maf*$^{-/-}$ fetal livers and counted the number of erythroblasts associated with each single central macrophage according to a previously described method.[7]

Interestingly, although more than ten Ter119-positive erythroblasts were adhered to a F4/80 positive macrophage in *c-Maf*$^{+/+}$ fetal livers, c-Maf-deficient central macrophages seemed to harbor far fewer erythroblasts (Figure 7). As shown in Figure 7A, the number of erythroblasts attached to a single central macrophage was significantly reduced in *c-Maf*$^{-/-}$ erythroblastic islands (14.2±0.3 and 5.6±1.5 erythroblasts per macrophage for *c-Maf*$^{+/+}$ and *c-Maf*$^{-/-}$, respectively). This result clearly indicates that erythroblastic island formation is impaired in the *c-Maf*$^{-/-}$ fetal livers.

Next, to address whether c-Maf-deficiency in macrophages was particularly responsible for the impairment of erythroblastic island formation, we performed a series of reconstitution experiments. After attaching the native erythroblastic island either from *c-Maf*$^{+/+}$ or *c-Maf*$^{-/-}$ fetal livers on a glass coverslip, the adherent erythroblasts in islands were stripped from macrophages. Then, the freshly isolated erythroblasts from *c-Maf*$^{+/+}$ or *c-Maf*$^{-/-}$ fetal livers were co-cultured on the remaining

adherent *c-Maf*$^{+/+}$ or *c-Maf*$^{-/-}$ fetal liver macrophages, respectively, so that *c-Maf*$^{+/+}$ erythroblast were co-cultured on *c-Maf*$^{-/-}$ central macrophages and *vice versa*. Surprisingly, *c-Maf*$^{-/-}$ macrophages failed to support erythroblastic island formation with the inoculated wild-type erythroblasts (12.7±0.5 erythroblasts per *c-Maf*$^{+/+}$ macrophage and 4.8±0.2 erythroblasts per *c-Maf*$^{-/-}$ macrophage; Figure 7B). In contrast, *c-Maf*$^{-/-}$ erythroblasts were still capable of attaching to *c-Maf*$^{+/+}$ macrophages as wild-type erythroblasts (13.9±0.5 erythroblasts per *c-Maf*$^{+/+}$ macrophage and 5.1±0.4 erythroblasts per *c-Maf*$^{-/-}$ macrophage; Figure 7C). These results demonstrate that the erythropoietic defects in *c-Maf*$^{-/-}$ embryos could be induced by an impaired hematopoietic microenvironment. Most likely, the suppressed functions of c-Maf-deficient central macrophages are responsible for the damaged erythroblastic islands.

3-6. Identification of target genes of c-Maf in fetal liver macrophages.

To identify the molecular targets by which c-Maf regulates formation of erythroblastic islands in macrophages, we monitored expression of cell adhesion molecules by microarray analysis. The expression of several important adhesion molecules was decreased in *c-Maf*$^{-/-}$ macrophages (Table 3). Expression of VCAM-1 was suppressed the furthest in these molecules. To confirm the results from microarray analysis, we performed quantitative RT-PCR analyses, examining expression levels of VCAM-1, Integrin alpha V, and Erythroblast Macrophage Protein (EMP). These three molecules are essential for erythroblastic islands formation, and are thus designated as Erythroblast-macrophage adhesive molecules.[4] The Mac-1 positive cells from either E13.5 or E14.5

fetal liver were sorted by MACS™ and analyzed for mRNA abundance of these genes by real time RT-PCR analysis. Of note, we observed an approximately two-fold reduction in the VCAM-1 mRNA expression level in the Mac-1 positive fraction from *c-Maf*$^{-/-}$ fetal liver, compared with the *c-Maf*$^{+/+}$ control at E13.5 and E14.5 (Figure 8A-B). However, Integrin alpha V and EMP mRNA expression were not significantly different between *c-Maf*$^{+/+}$ and *c-Maf*$^{-/-}$ (Figure 8A-B). Consistent with this observation, flow cytometry analysis of the fetal liver cells also verified a significant reduction of VCAM-1 positive cells in the *c-Maf*$^{-/-}$ fetal liver Mac-1 positive cells (20.1±4.0%: Figure 8C, right panel) compared to the *c-Maf*$^{+/+}$ fetal liver Mac-1 positive cells (28.4±1.5%; Figure 8C, left panel).

Given the significant suppression of VCAM-1 expression in *c-Maf*$^{-/-}$ fetal liver macrophages, we next addressed whether c-Maf could activate the *VCAM-1* gene promoter. To this end, we performed a transfection assay in the RAW264.7 macrophage cell line, using the -0.7 kilobase (kb) *VCAM-1* promoter region, which was joined to the 5' end of the firefly luciferase reporter gene. Interestingly, the *VCAM-1* promoter reporter was activated upon co-expression with the c-Maf expression plasmid (pEFX3-FLAG-c-Maf), in a c-Maf dose dependent manner (Figure 8D). Furthermore, sequence analysis using the TRANSFAC database identified two putative half MARE sites at 5' -318bp and -136bp from the mouse *VCAM-1* gene promoter. Overall, these data suggest that c-Maf may directly regulate the expression of *VCAM-1* by binding the half-MARE site in its promoter region.

4. Discussion

Macrophages are important for hematopoiesis because they engulf nuclei of erythroblasts in erythroblastic islands, where the macrophages are surrounded by erythroblasts in the fetal liver, bone marrow and spleen.[4] In the present study, we investigated deficiencies of the transcription factor c-Maf caused by embryonic anemia resulting from failure to form erythroblastic islands, as reflected by a defective adhesive function of fetal liver macrophages. Our main conclusion is that c-Maf is indispensable for the function of macrophages in erythropoiesis.

Our study clearly demonstrates that disruption of c-Maf causes impairment of erythroblastic islands formation due to dysfunction of fetal liver macrophages. In a methylcellulose culture system, *c-Maf*$^{-/-}$ hematopoietic stem/progenitor cells in fetal liver have a normal potential to differentiate into different lineages, and they can reconstitute the hematopoietic system of lethally irradiated mice. Because c-Maf is specifically expressed in macrophages within the fetal liver, it has been thought that c-Maf doesn't regulate fetal liver erythropoiesis through a function of erythroblasts, but rather it performs an adhesive function of macrophages. There are several reports about genes that are related to the formation of erythroblastic islands, based on the knockout mice technique. Retinoblastoma deficient mice were analyzed for macrophage differentiation, and erythroblastic islands formation was reported to be impaired in these mice.[7] The fetal livers of *Dnase2a*$^{-/-}$ mice contain many macrophages carrying undigested DNA, and interferon-β mRNA was expressed by the resident macrophages in the *Dnase2a*$^{-/-}$ fetal liver.[36,37] In *c-Maf*$^{-/-}$ fetal livers, Retinoblastoma was comparably expressed in *c-Maf*$^{+/+}$ and *c-Maf*$^{-/-}$ macrophages, therefore impaired erythroblastic

islands formation in *c-Maf*$^{-/-}$ mice is not related to Retinoblastoma (supplemental Figure 4). In addition, we could not detect the abnormal foci that are found in *Dnase2a*$^{-/-}$ fetal livers or the expression of interferon-β mRNA (Data not shown). Thus Retinoblastoma or DNase II do not cause the lethality of *c-Maf*$^{-/-}$ embryos.

To identify the target genes of c-Maf in fetal liver macrophages, we performed microarray analysis and found VCAM-1 was one of these target genes. VCAM-1 is known as an adhesion molecule expressed on macrophages of erythroblastic islands. Previous studies revealed that the formation of erythroblastic islands was impaired by the anti-VCAM-1 antibody.[10,38] As shown in Figure 5, mRNA of *VCAM-1* was decreased in *c-Maf*$^{-/-}$ fetal liver macrophages. This suggests that decreased expression of *VCAM-1* may be at least in part responsible for impaired erythroblastic islands formation in *c-Maf*$^{-/-}$ fetal liver. The large Maf proteins are known to bind Maf recognition elements (MAREs) or the 5' AT-rich half MARE. In the *VCAM-1* promoter region, there is a half-MARE site 318bp and 136bp from the transcription start site, so c-Maf may directly regulate *VCAM-1* expression in fetal liver macrophages. Recently, Kohyama et al. revealed that Spi-C controls the development of red pulp macrophages required for red blood cell recycling, and it regulates *VCAM-1* expression in red pulp macrophages.[39] These earlier results and ours suggest that the regulation of *VCAM-1* expression by transcription factors strongly affects the function of tissue macrophages. We previously reported that c-Maf regulates F4/80 expression[30], and in the present study we demonstrate that c-Maf regulates VCAM-1 expression. In macrophages, c-Maf regulates the expression of cell surface molecules that are involved in macrophage function.

We found that c-Maf is indispensable for erythroblastic island formation in the embryonic stage, but this was not the case for the adult stage. In a reconstitution assay using fetal liver cells, *c-Maf*$^{-/-}$ hematopoietic cells reconstituted hematopoiesis of lethally irradiated mice, and the mice that were transplanted with *c-Maf*$^{-/-}$ fetal liver cells did not show anemia. These results indicate that the importance of erythroblastic islands is not the same in the embryonic versus adult stage. This hypothesis is supported by previous observations. In *Palld* $^{-/-}$ fetal liver, erythroblastic islands formation was impaired, but *Palld*$^{-/-}$ fetal liver cells could reconstitute the blood of lethally irradiated mice.[8] Thus, c-Maf and Palladin are important for hematopoiesis only in the embryonic stage. On the other hand, a previous study found that ICAM-4 is critical in erythroblastic islands formation in adult marrow, but ICAM-4 knockout mice did not show anemia in the embryonic stage. This result indicates that ICAM-4 is important for hematopoiesis only in the adult stage.[40] Overall, the data indicate that there might be different mechanisms between fetal liver and adult marrow/spleen erythroblastic islands formation.

Recent reports have indicated that definitive as well as primitive erythropoiesis are related to erythroblastic islands.[38] Kingsley et al. revealed that yolk sac-derived primitive erythroblasts enucleate during gestation[41] and Isern et al. also demonstrated, using transgenic mouse lines, that primitive erythroblasts enucleate within the fetal liver.[38,42] Our quantitative RT-PCR results suggested that definitive erythropoiesis is more involved in erythroblastic islands formation than is primitive erythropoiesis *in vivo* (Figure 4). Therefore, this result indicates that definitive erythropoiesis in fetal liver is predominantly impaired in *c-Maf*$^{-/-}$ embryos, whereas primitive

erythropoiesis is maintained in *c-Maf*$^{-/-}$ embryos.

Our study demonstrated that *c-Maf*$^{-/-}$ mice were embryonic lethal on the C57BL/6 background and that *c-Maf*$^{-/-}$ macrophages were responsible for this. Previous reports from our laboratory and from others indicated that *c-Maf*$^{-/-}$ mice were lethal around birth on C57BL/6Jx129/SV or BALB/c backgrounds.[16,43,44] It is known that the cytokine production in T helper cells differs between C57BL/6 and BALB/c backgrounds. Recently Mills at al. reported that cytokine production in macrophages differed according to the backgrounds of the mice.[45] On a C57BL/6 background, inflammatory cytokine production is more dominant than on a BALB/c background. Therefore our *c-Maf*$^{-/-}$ mice were lethal at an earlier gestational date than indicated by previous reports. We found that *c-Maf*$^{-/-}$ fetal liver macrophages produced more cytokines than *c-Maf*$^{+/+}$ fetal liver macrophages (Figure 9). This finding supports the idea that the *c-Maf*$^{-/-}$ macrophages are responsible for anemia and lethality. This hypothesis may also explain the phenotype discrepancy between *c-Maf*$^{-/-}$ mice and *F4/80*$^{-/-}$ or *VCAM-1*$^{-/-}$ mice. Neither F4/80 knockout mice nor mice with a conditional ablation of VCAM-1 in blood cells are embryonic lethal.[46-48] Our results indicate that increased apoptotic red blood cells in *c-Maf*$^{-/-}$ fetal liver is thought to be trigger inflammatory cytokine production, and these cytokines may induce a secondary cause of embryonic lethality on the C57BL/6 background.

In summary, we have shown that the transcription factor c-Maf gene affects the hematopoietic microenvironment by playing a crucial role in fetal liver macrophages.

5. Acknowledgements

I would like to thank Professor Satoru Takahashi, Professor Haruhiko Ninomiya, Professor Shigeru Chiba and Dr. Michito Hamada for giving me the opportunity for carrying out this research, and for their guidance and supervisions throughout my post graduate research training.

I would also like to thank Associate Professor Takashi Kudo, Assistant Professor Masatsugu Ema for their guidance and for invaluable advice, support and encouragement through out my research project.

Finally, I also thank my colleagues in the Department of Anatomy and Embryology, University of Tsukuba.

6. References

1. Palis J. Ontogeny of erythropoiesis. Curr Opin Hematol. 2008;15:155-161.

2. Allen TD, Dexter TM. Ultrastructural aspects of erythropoietic differentiation in long-term bone marrow culture. Differentiation. 1982;21:86-94.

3. Bessis M. [Erythroblastic island, functional unity of bone marrow.]. Rev Hematol. 1958;13:8-11.

4. Chasis JA, Mohandas N. Erythroblastic islands: niches for erythropoiesis. Blood. 2008;112:470-478.

5. Hanspal M, Hanspal JS. The association of erythroblasts with macrophages promotes erythroid proliferation and maturation: a 30-kD heparin-binding protein is involved in this contact. Blood. 1994;84:3494-3504.

6. Mohandas N, Prenant M. Three-dimensional model of bone marrow. Blood. 1978;51:633-643.

7. Iavarone A, King ER, Dai X-M, Leone G, Stanley ER, Lasorella A. Retinoblastoma promotes definitive erythropoiesis by repressing Id2 in fetal liver macrophages. Nature. 2004;432:1040-1045.

8. Liu X-S, Li X-H, Wang Y, et al. Disruption of palladin leads to defects in definitive erythropoiesis by interfering with erythroblastic island formation in mouse fetal liver. Blood. 2007;110:870-876.

9. Soni S, Bala S, Gwynn B, Sahr KE, Peters LL, Hanspal M. Absence of erythroblast macrophage protein (Emp) leads to failure of erythroblast nuclear extrusion. J Biol Chem. 2006;281:20181-20189.

10. Sadahira Y, Yoshino T, Monobe Y. Very late activation antigen 4-vascular cell adhesion molecule 1 interaction is involved in the formation of erythroblastic islands. J Exp Med. 1995;181:411-415.

11. Nishizawa M, Kataoka K, Goto N, Fujiwara KT, Kawai S. v-maf, a viral oncogene that encodes a "leucine zipper" motif. Proc Natl Acad Sci USA. 1989;86:7711-7715.

12. Kataoka K, Fujiwara KT, Noda M, Nishizawa M. MafB, a new Maf family transcription activator that can

associate with Maf and Fos but not with Jun. Mol Cell Biol. 1994;14:7581-7591.

13. Kataoka K, Noda M, Nishizawa M. Maf nuclear oncoprotein recognizes sequences related to an AP-1 site and forms heterodimers with both Fos and Jun. Mol Cell Biol. 1994;14:700-712.

14. Yoshida T, Ohkumo T, Ishibashi S, Yasuda K. The 5'-AT-rich half-site of Maf recognition element: a functional target for bZIP transcription factor Maf. Nucleic Acids Res. 2005;33:3465-3478.

15. Kajihara M, Kawauchi S, Kobayashi M, Ogino H, Takahashi S, Yasuda K. Isolation, characterization, and expression analysis of zebrafish large Mafs. J Biochem. 2001;129:139-146.

16. Kawauchi S, Takahashi S, Nakajima O, et al. Regulation of lens fiber cell differentiation by transcription factor c-Maf. J Biol Chem. 1999;274:19254-19260.

17. Moriguchi T, Hamada M, Morito N, et al. MafB is essential for renal development and F4/80 expression in macrophages. Mol Cell Biol. 2006;26:5715-5727.

18. Ogino H, Yasuda K. Induction of lens differentiation by activation of a bZIP transcription factor, L-Maf. Science. 1998;280:115-118.

19. Sieweke MH, Tekotte H, Frampton J, Graf T. MafB is an interaction partner and repressor of Ets-1 that inhibits erythroid differentiation. Cell. 1996;85:49-60.

20. Swaroop A, Xu JZ, Pawar H, Jackson A, Skolnick C, Agarwal N. A conserved retina-specific gene encodes a basic motif/leucine zipper domain. Proc Natl Acad Sci USA. 1992;89:266-270.

21. Zhang C, Moriguchi T, Kajihara M, et al. MafA is a key regulator of glucose-stimulated insulin secretion. Mol Cell Biol. 2005;25:4969-4976.

22. Eychene A, Rocques N, Pouponnot C. A new MAFia in cancer. Nat Rev Cancer. 2008;8:683-693.

23. Hurt EM, Wiestner A, Rosenwald A, et al. Overexpression of c-maf is a frequent oncogenic event in multiple myeloma that promotes proliferation and pathological interactions with bone marrow stroma. Cancer Cell. 2004;5:191-199.

24. Morito N, Yoh K, Fujioka Y, et al. Overexpression of c-Maf contributes to T-cell lymphoma in both mice and human. Cancer Res. 2006;66:812-819.

25. Murakami YI, Yatabe Y, Sakaguchi T, et al. c-Maf expression in angioimmunoblastic T-cell lymphoma. Am J Surg Pathol. 2007;31:1695-1702.

26. Bauquet AT, Jin H, Paterson AM, et al. The costimulatory molecule ICOS regulates the expression of c-Maf and IL-21 in the development of follicular T helper cells and TH-17 cells. Nat Immunol. 2009;10:167-175.

27. Ho IC, Hodge MR, Rooney JW, Glimcher LH. The proto-oncogene c-maf is responsible for tissue-specific expression of interleukin-4. Cell. 1996;85:973-983.

28. Cao S, Liu J, Song L, Ma X. The protooncogene c-Maf is an essential transcription factor for IL-10 gene expression in macrophages. J Immunol. 2005;174:3484-3492.

29. Aziz A, Soucie E, Sarrazin S, Sieweke MH. MafB/c-Maf deficiency enables self-renewal of differentiated functional macrophages. Science. 2009;326:867-871.

30. Nakamura M, Hamada M, Hasegawa K, et al. c-Maf is essential for the F4/80 expression in macrophages in vivo. Gene. 2009;445:66-72.

31. Masuoka HC, Townes TM. Targeted disruption of the activating transcription factor 4 gene results in severe fetal anemia in mice. Blood. 2002;99:736-745.

32. Atarashi K, Nishimura J, Shima T, et al. ATP drives lamina propria T(H)17 cell differentiation. Nature.

2008;455:808-812.

33. Sankaran VG, Xu J, Ragoczy T, et al. Developmental and species-divergent globin switching are driven by BCL11A. Nature. 2009;460:1093-1097.

34. Yamashita T, Ohneda O, Sakiyama A, Iwata F, Ohneda K, Fujii-Kuriyama Y. The microenvironment for erythropoiesis is regulated by HIF-2alpha through VCAM-1 in endothelial cells. Blood. 2008;112:1482-1492.

35. Zhang J, Socolovsky M, Gross AW, Lodish HF. Role of Ras signaling in erythroid differentiation of mouse fetal liver cells: functional analysis by a flow cytometry-based novel culture system. Blood. 2003;102:3938-3946.

36. Kawane K, Fukuyama H, Kondoh G, et al. Requirement of DNase II for definitive erythropoiesis in the mouse fetal liver. Science. 2001;292:1546-1549.

37. Yoshida H, Okabe Y, Kawane K, Fukuyama H, Nagata S. Lethal anemia caused by interferon-beta produced in mouse embryos carrying undigested DNA. Nat Immunol. 2005;6:49-56.

38. Isern J, Fraser ST, He Z, Baron MH. The fetal liver is a niche for maturation of primitive erythroid cells. Proc Natl Acad Sci U S A. 2008;105:6662-6667.

39. Kohyama M, Ise W, Edelson BT, et al. Role for Spi-C in the development of red pulp macrophages and splenic iron homeostasis. Nature. 2009;457:318-321.

40. Lee G, Lo A, Short SA, et al. Targeted gene deletion demonstrates that the cell adhesion molecule ICAM-4 is critical for erythroblastic island formation. Blood. 2006;108:2064-2071.

41. Kingsley PD, Malik J, Fantauzzo KA, Palis J. Yolk sac-derived primitive erythroblasts enucleate during mammalian embryogenesis. Blood. 2004;104:19-25.

42. Fraser ST, Isern J, Baron MH. Maturation and enucleation of primitive erythroblasts during mouse

embryogenesis is accompanied by changes in cell-surface antigen expression. Blood. 2007;109:343-352.

43. Kim JI, Li T, Ho IC, Grusby MJ, Glimcher LH. Requirement for the c-Maf transcription factor in crystallin gene regulation and lens development. Proc Natl Acad Sci U S A. 1999;96:3781-3785.

44. Ring BZ, Cordes SP, Overbeek PA, Barsh GS. Regulation of mouse lens fiber cell development and differentiation by the Maf gene. Development. 2000;127:307-317.

45. Mills CD, Kincaid K, Alt JM, Heilman MJ, Hill AM. M-1/M-2 macrophages and the Th1/Th2 paradigm. J Immunol. 2000;164:6166-6173.

46. Lin HH, Faunce DE, Stacey M, et al. The macrophage F4/80 receptor is required for the induction of antigen-specific efferent regulatory T cells in peripheral tolerance. J Exp Med. 2005;201:1615-1625.

47. Schaller E, Macfarlane AJ, Rupec RA, Gordon S, McKnight AJ, Pfeffer K. Inactivation of the F4/80 glycoprotein in the mouse germ line. Mol Cell Biol. 2002;22:8035-8043.

48. Ulyanova T, Scott LM, Priestley GV, et al. VCAM-1 expression in adult hematopoietic and nonhematopoietic cells is controlled by tissue-inductive signals and reflects their developmental origin. Blood. 2005;106:86-94.

7. Tables

Table 1. Genotypic analysis of neonates and embryos from ***c-Maf*** $^{+/-}$ intercross on a C57BL/6J back ground.

Embryonic stage	Number of each ***c-Maf*** genotype			Total numbers of embryos
	c-Maf $^{+/+}$	***c-Maf*** $^{+/-}$	***c-Maf*** $^{-/-}$	
E12.5	12	20	10	42
E13.5*	20	35	16 (3)	71
E14.5*	42	47	30 (7)	119
E15.5*	16	40	15 (2)	71
E16.5*	11	15	4 (3)	30
E18.5*	9	12	3 (2)	24
Neonate	13	29	0	42

Embryos were isolated at the indicated time points of gestation and within 7 days of birth (postnatal), and analyzed for viability. Genotypes of embryos were determined by PCR. *Parentheses indicate number of dead embryos.

Table 2. Blood cell counts 10-12 weeks after fetal liver cell transplantation in mice.

Genotype of transplanted FLC	***c-Maf*** $^{+/+}$	***c-Maf*** $^{-/-}$	*p* value
WBC, /ml	18,200±1,880	17,800±1,240	NS
RBC, x10^4/ ml	968±7.5	944±8.1	p =0.04
Hb, g/dl	14.9±0.5	13.8±0.1	p =0.04
HCT, %	46.6±0.5	45.5±0.3	NS
MCV, fl	48.1±0.3	48.2±0.3	NS
MCH, pg	15.4±0.5	14.6±0.1	NS
PLT, x10^4/ ml	111.6±4.2	99.6±3.6	p =0.04

Values shown are the mean ± SEM (Standard Error of the Mean) for 12 mice per genotype. FLC, fetal liver cell; WBC, white blood cell; RBC, red blood cell; Hb, hemoglobin; HCT, hematocrit; MCV, mean corpuscular volume; MCH, mean corpuscular hemoglobin; PLT, platelet; NS, not significant.

Table 3. Expression of genes involved in macrophage signature

		c-Maf $^{+/+}$	***c-Maf*** $^{-/-}$	
Symbol	**Official Full Name**	**Signal**	**Signal**	**'Fold'**
VCAM-1	vascular cell adhesion molecule 1	8.3	1.6	0.19
Mrc1	mannose receptor, C type 1	19.8	5.7	0.29
Csf1r	colony stimulating factor 1 receptor	45	16.8	0.37
Sell	selectin, lymphocyte	26.7	10	0.37
Lamp2	lysosomal-associated membrane protein 2	8.9	3.3	0.37
Itgav	Integrin alpha V	1.2	0.5	0.41
Maea (EMP)	macrophage erythroblast attacher	26.2	14.5	0.55
Emr1 (F4/80)	EGF-like module containing, mucin-like, hormone receptor-like sequence 1	71.4	48.1	0.67
Itgam (Mac-1)	integrin alpha M	5.8	3.9	0.67
Cd163	CD163 antigen	0.6	0.4	0.67
Cd14	CD14 antigen	11.8	9.4	0.80
Fcgr1	Fc receptor, IgG, high affinity I	15.7	17.6	1.12

Fetal liver macrophages were purified by flow cytometry from ***c-Maf*** $^{+/+}$ or ***c-Maf*** $^{-/-}$ fetal livers. The 'fold change' in the gene expression was determined by dividing the signal obtained with ***c-Maf*** $^{-/-}$ fetal liver macrophage RNA by the signal obtained with ***c-Maf*** $^{+/+}$ RNA.

8. Figure Legends

Figure 1. *c-Maf*$^{-/-}$ embryos show anemia.

(A) Gross appearance of E13.5 embryos. The *c-Maf*$^{-/-}$ embryo is paler and smaller than its *c-Maf*$^{+/+}$ littermate. Scale bar represents 5mm. (B) Hematocrit values for *c-Maf*$^{+/+}$ (n=6) and *c-Maf*$^{-/-}$ (n=6) at E13.5 embryos, *c-Maf*$^{+/+}$ (n=8) and *c-Maf*$^{-/-}$ (n=7) at E14.5 embryos, *c-Maf*$^{+/+}$ (n=12) and *c-Maf*$^{-/-}$ (n=9) at E15.5 embryos. Data are presented as mean ±SEM. The mean hematocrit values for *c-Maf*$^{-/-}$ embryos were significantly lower than those for *c-Maf*$^{+/+}$ at E13.5, E14.5 and E15.5. (C) Blood smears from E13.5 embryos stained with May-Grünwald-Giemsa stain. The blood smear from a *c-Maf*$^{-/-}$ embryo contains far fewer enucleated red blood cells. Scale bars represent 20μm. (D) The percentage of enucleated red blood cells in peripheral blood for *c-Maf*$^{+/+}$ (n=5) and *c-Maf*$^{-/-}$ (n=7) at E13.5 embryos, *c-Maf*$^{+/+}$ (n=4) and *c-Maf*$^{-/-}$ (n=4) at E14.5 embryos, *c-Maf*$^{+/+}$ (n=8) and *c-Maf*$^{-/-}$ (n=8) at E15.5 embryos. Data are presented as mean ±SEM. The percentage of enucleated red blood cells is significantly reduced in *c-Maf*$^{-/-}$ embryos as compared with *c-Maf*$^{+/+}$ embryos at E13.5, E14.5 and E15.5. *$p< 0.05$, **$p< 0.01$.

Figure 2. Increased number of apoptotic cells is observed in *c-Maf*$^{-/-}$ fetal liver.

(A) Gross appearance of E13.5 fetal liver. The *c-Maf*$^{-/-}$ fetal liver is smaller than a wild-type fetal liver. Scale bar represents 100μm. (B) the mean total number of fetal liver cells in *c-Maf*$^{+/+}$ (n=14) and *c-Maf*$^{-/-}$ (n=10) at E13.5 embryos, *c-Maf*$^{+/+}$ (n=6) and *c-Maf*$^{-/-}$ (n=4) at E14.5 embryos, *c-Maf*$^{+/+}$ (n=8) and *c-Maf*$^{-/-}$ (n=8) at E15.5 embryos,. The mean number of fetal liver cells is significantly

reduced in *c-Maf*$^{-/-}$ embryos. Data are presented as mean ±SEM. (C) Hematoxin and Eosin staining of *c-Maf*$^{+/-}$ and *c-Maf*$^{-/-}$ fetal liver sections (Upper panel). TUNEL assay shows increased apoptosis in *c-Maf*$^{-/-}$ fetal liver (middle and lower panel). Scale bars in upper and middle panel represent 200μm. Scale bars in lower panel represent 50μm. (D) The fraction of cells in different phases of the cell cycle was measured by propidium iodide (PI) staining followed by flow cytometric analyses. Typical flow cytometric profiles of *c-Maf*$^{+/+}$ and *c-Maf*$^{-/-}$ fetal liver cells isolated from E12.5 embryos are shown. The percentage of cells in sub-G_1, G_1, S phase, and G_2/M are indicated. The sub-G_1 represents the apoptotic population. The apoptotic population was increased in *c-Maf*$^{-/-}$ fetal liver. □ represents *c-Maf*$^{+/+}$; ■ represents *c-Maf*$^{-/-}$. n = 3 per group; *p<0.05. Data are presented as mean ±SEM.

Figure 3. Definitive erythropoiesis in fetal liver is impaired in *c-Maf*$^{-/-}$ embryos but *c-Maf*$^{-/-}$ fetal liver cells can form erythroid colonies.

(A) Typical flow cytometric profiles of *c-Maf*$^{+/+}$ and *c-Maf*$^{-/-}$ fetal liver cells isolated from E13.5 embryos double labeled with a FITC-conjugated anti-CD71 monoclonal antibody (mAb) and a APC-conjugated anti-TER-119 mAb. Regions R1 to R5 are defined by a characteristic staining pattern of cells as indicated. The mean percentages for the populations in each region are shown in red. (B) Comparison of *c-Maf*$^{+/+}$ and *c-Maf*$^{-/-}$ fetal livers in the ratio of R1 to R5. □ represents *c-Maf*$^{+/+}$; ■ represents *c-Maf*$^{-/-}$. n = 5~7 per group; *p<0.05. (C) The ratio of annexin V positive cells from R1 to R5 was compared in *c-Maf*$^{+/+}$ and *c-Maf*$^{-/-}$ fetal livers. □ represents *c-Maf*$^{+/+}$; ■

represents *c-Maf*$^{-/-}$. n = 5~7 per group; *p<0.05. (D) Cytospin preparation from *c-Maf*$^{+/+}$ and *c-Maf*$^{-/-}$ fetal liver single cells stained with May-Grünwald Giemsa. Mature red blood cells (R4 to R5) were reduced in *c-Maf*$^{-/-}$ fetal liver as compared with *c-Maf*$^{+/+}$ fetal liver. Arrows indicate R4 and R5 population. (E) *In vitro* colony assay using fetal liver cells from *c-Maf*$^{+/+}$ (□) and *c-Maf*$^{-/-}$ (■) embryos. A total of 20, 000 fetal liver cells were plated and cultured with methylcellulose media. The numbers of CFU-E, BFU-E and CFU-GEMM derived colonies are shown. The number of CFU-E derived colonies was significantly increased in *c-Maf*$^{-/-}$ embryos. There was no significant difference between the number of BFU-E and CFU-GEMM derived colonies in *c-Maf*$^{+/+}$ (□) and *c-Maf*$^{-/-}$ (■) embryos. n = 6~7 per group; *p<0.05. Data are presented as mean ±SEM. CFU-E: Colony-forming unit-erythroid, BFU-E: Burst-forming unit-erythroid, CFU-GEMM: Colony-forming unit-granulocyte, erythroid, macrophage, megakaryocyte,

Figure 4. Decreased mRNA expression of βmajor/βminor globins in *c-Maf*$^{-/-}$ fetal liver.

Mac-1 negative fraction was isolated by Mac-1 magnetic beads. Analyses of mRNA expression of mouse β-globin chains showed that mRNA expression of βmajor/βminor globins was decreased, whereas embryonic β-globin genes (εy-globin and βh1-globin) are maintained in Mac-1 negative fraction in E13.5 *c-Maf*$^{-/-}$ fetal liver cells. □ represents *c-Maf*$^{+/+}$; ■ represents *c-Maf*$^{-/-}$. n=7 per group. *p<0.01. Data are presented as mean ±SEM.

Figure 5. The *in vitro* erythroid colony formation of *c-Maf*$^{-/-}$ fetal liver cells is not impaired.

(A) Hemoglobin levels in day 2 CFU-Es from *c-Maf*$^{+/+}$ and *c-Maf*$^{-/-}$ E13.5 fetal liver cells are shown. (B) Cytospun cells from day 2 CFU-Es (from E13.5 fetal liver cells in *c-Maf*$^{+/+}$ upper panel, and *c-Maf*$^{-/-}$; lower panel) are stained with May-Grünwald Giemsa. Note enucleated red blood cells are observed in cytospin picked from *c-Maf*$^{-/-}$ CFU-Es. The scale bar represents 20μm.

Figure 6. *c-Maf*$^{-/-}$ fetal liver cells can reconstitute adult hematopoiesis in lethally irradiated mice.

(A) 2 ×10^6 E14.5 fetal liver cells from *c-Maf*$^{+/+}$ or *c-Maf*$^{-/-}$ embryos were injected into lethally irradiated recipient mice. After 8-10 weeks following transplantation, the donor leukocyte chimerism of the mice reconstituted with *c-Maf*$^{-/-}$ fetal liver cells was comparable with that of the mice reconstituted with *c-Maf*$^{+/+}$ fetal liver cells. The reconstitution efficiency was checked with the Ly5.2/Ly5.2 ratio of peripheral blood cells by flow cytometry. Donor chimerism was determined to be: [%Ly5.1$^+$ / %Ly5.1$^+$ + %Ly5.2$^+$] × 100. (B) No significant difference was found in the proportion of each lineage in peripheral blood between *c-Maf*$^{+/+}$ fetal liver cells-transplanted mice and *c-Maf*$^{-/-}$ fetal liver cells-transplanted mice. (C and D) Left: Flow cytometric analyses of the expression of TER-119 and CD71 in total bone marrow cells prepared from femur of *c-Maf*$^{+/+}$ fetal liver cells transplanted (left panels) and *c-Maf*$^{-/-}$ fetal liver cells transplanted (center panels) mice. Frequencies (%) of cells in gated fractions (squared) are shown. In the right panels, frequencies (%) of CD71+/TER-119- (top left region: Q1), CD71+/TER-119+ (top right region: Q2) and CD71-/TER-119+ (bottom right region: Q3) cells in bone marrow are also indicated. Right:

Frequencies (%) of CD71/TER-119 cells (gated fractions of the left panels). □ represents *c-Maf*$^{+/+}$ fetal liver cells transplanted mice; ■ represents *c-Maf*$^{-/-}$ fetal liver cells transplanted mice. n=4 per group. (D) Left: Flow cytometric analyses of the expression of TER-119 and CD71 in total spleen cells prepared from *c-Maf*$^{+/+}$ fetal liver cells transplanted mice (left panels) and *c-Maf*$^{-/-}$ fetal liver cells transplanted mice (center panels). In the right panels, the frequencies (%) of CD71+ (top left and top right region: CD71+) and CD71-/TER-119+ (indicated squared gate in bottom right region: TER-119+) cells in spleen are also indicated. □ represents *c-Maf*$^{+/+}$ fetal liver cells transplanted mice; ■ represents *c-Maf*$^{-/-}$ fetal liver cells transplanted mice. n=4 per group. FLC, fetal liver cell;

Figure 7. Absence of c-Maf impairs the formation of erythroblastic islands in the fetal liver.

(A) Native erythroblastic islands isolated from *c-Maf*$^{+/+}$ and *c-Maf*$^{-/-}$ fetal liver were immunostained with F4/80 (Green) and TER-119 (Red) antibodies as described in Material and methods. F4/80 is used as a macrophage-specific marker, and Ter119 is used as a marker for erythroblasts. The number of erythroblasts surrounding each macrophage was significantly reduced in *c-Maf*$^{-/-}$ fetal liver. (B) Erythroblastic islands reconstituted with *c-Maf*$^{+/+}$ erythroblasts were immunostained with F4/80 (Green) and TER119 (Red) antibodies. The number of *c-Maf*$^{+/+}$ erythroblasts surrounding each *c-Maf*$^{-/-}$ macrophage was significantly reduced as compared with that seen for *c-Maf*$^{+/+}$ macrophages. (C) Erythroblastic islands reconstituted with *c-Maf*$^{-/-}$ erythroblasts were immunostained with F4/80 (Green) and TER119 (Red) antibodies. The number of *c-Maf*$^{-/-}$ erythroblasts surrounding each *c-Maf*$^{-/-}$ macrophage was significantly reduced compared with that

seen for *c-Maf*$^{+/+}$ macrophages. *c-Maf*$^{-/-}$ erythroblasts can form reconstituted erythroblastic islands with *c-Maf*$^{+/+}$ macrophage. However, *c-Maf*$^{-/-}$ macrophages showed impaired formation of reconstituted erythroblastic islands. The scale bar represents 20μm. n = 4~6 embryos per group. For each combination, at least 20 macrophages per embryo were analyzed. *p<0.05. Data are presented as mean ±SEM.

Figure 8. Decreased expression of VCAM-1 in *c-Maf*$^{-/-}$ fetal liver macrophage .

mRNA expression profiles of "Erythroblast-macrophage adhesive interaction" genes at E13.5(A) and at E14.5 (B). Total RNA obtained from Mac-1 positive fraction (gray bar) and Mac-1 negative fraction (open bar) of fetal liver cells was used for analyses. VCAM-1 expression was decreased in *c-Maf*$^{-/-}$ macrophages at E13.5 and E14.5. n = 7 per group; *p<0.05. All of the data are presented as mean ±SEM. (C) Representative histograms plotted after gating on Mac-1(CD11b) positive fraction from E13.5 fetal liver cells double labeled with a FITC-conjugated anti-Mac1(CD11b) mAb and a biotinylated anti-VCAM-1 mAb with APC conjugated streptavidin. *c-Maf*$^{-/-}$ fetal liver macrophages expressed a suppressed level of VCAM-1 compared with *c-Maf*$^{+/+}$ littermate controls. The bar graph shows that the percentage of VCAM-1 positive cells is decreased in *c-Maf*$^{-/-}$ fetal liver. (D) Schematic diagram of a luciferase reporter construct using a VCAM-1-0.7 kb promoter (VCAM-1-Luc) ligated to a firefly luciferase cassette. Two putative half MARE sites (5' -318bp and -136bp) are indicated. The pEFX3-FLAG-cMaf (10 ng or 40 ng per well) expression vectors were co-transfected with the reporter plasmid into the macrophage cell line RAW264.7. The relative

luciferase activity shown is derived from averages of 2 independent experiments (as mean ±SEM). The luciferase activity seen in RAW264.7 cells transfected with the reporter plasmid and with an empty vector was normalized to a value of 1 as the standard (*p<0.05).

Figure 9. *c-Maf*$^{-/-}$ fetal liver macrophage mRNA expression profiles

mRNA expression profiles of Rb and inflammatory cytokines. The population enriched for the Mac1-negative cells (open bar) and Mac1-positive cells (gray bar). n=7 per group. *p<0.05. Data are presented as mean ±SEM.

Figure 1

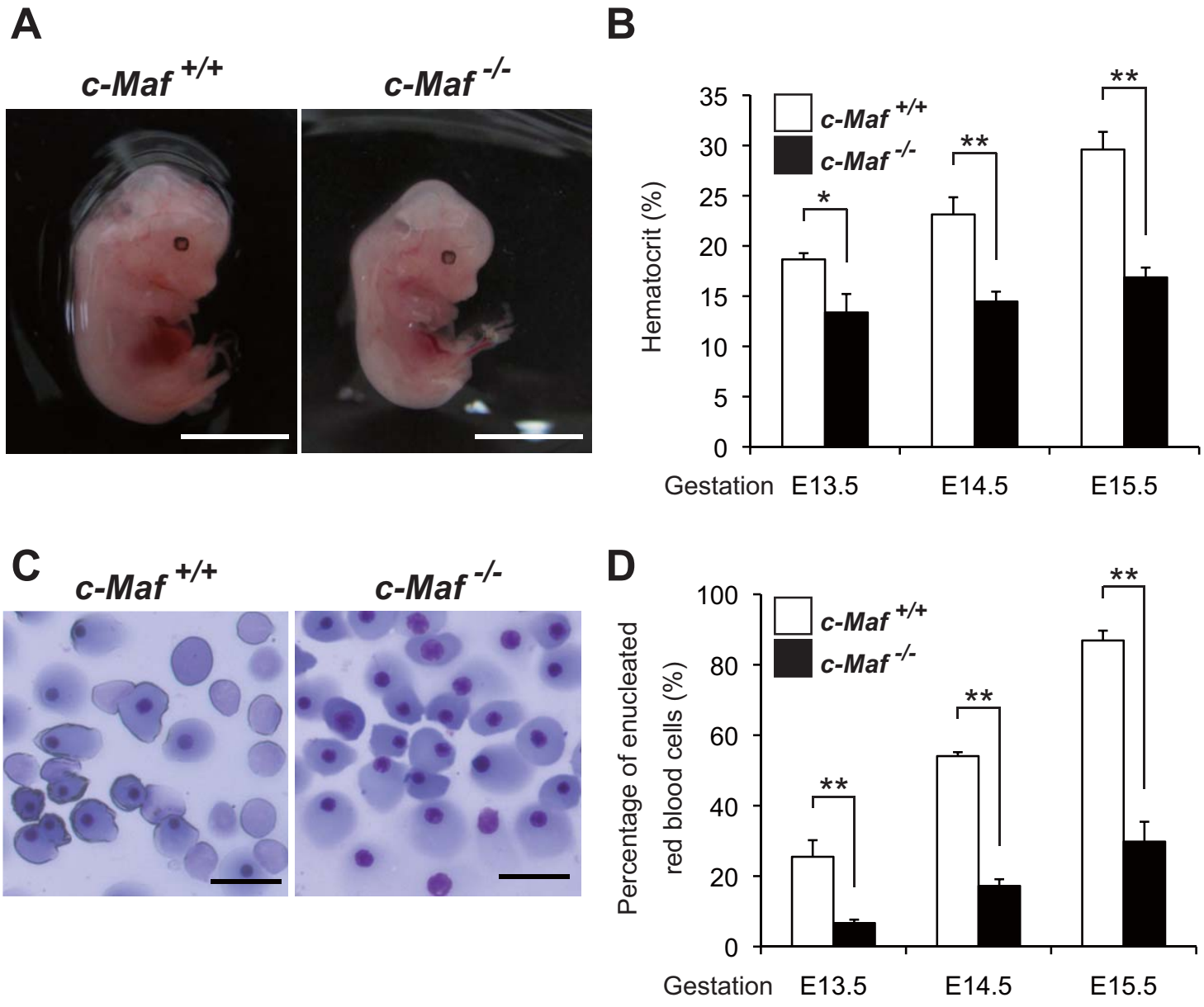
A
c-Maf +/+
c-Maf -/-
B
Hematocrit (%)
35
30
25
20
15
10
5
0
c-Maf +/+
c-Maf -/-
*
**
**
Gestation E13.5 E14.5 E15.5
C
c-Maf +/+
c-Maf -/-
D
Percentage of enucleated red blood cells (%)
100
80
60
40
20
0
c-Maf +/+
c-Maf -/-
**
**
**
Gestation E13.5 E14.5 E15.5

Figure 2

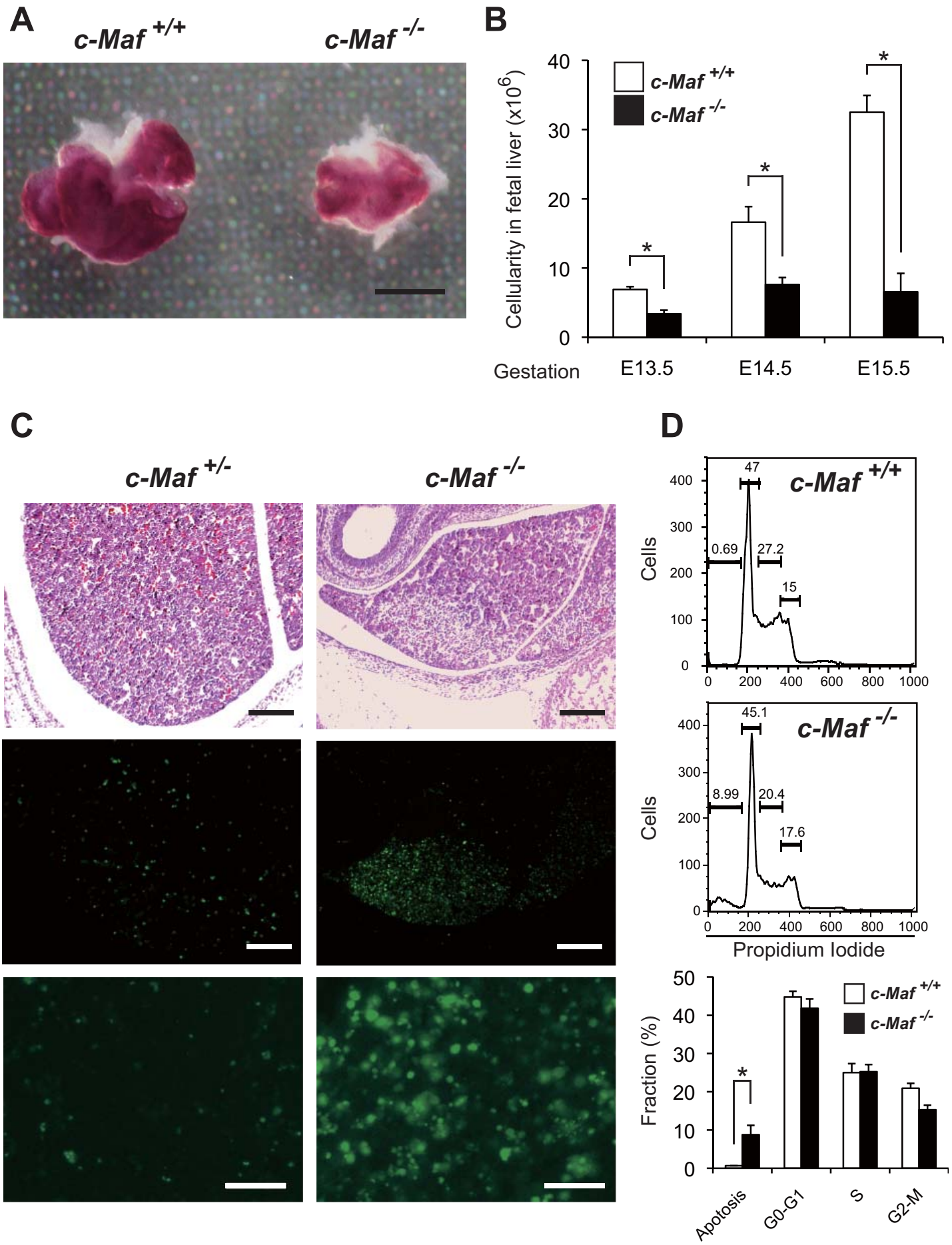
A
c-Maf +/+
c-Maf -/-
B
Cellularity in fetal liver (x10^6)
c-Maf +/+
c-Maf -/-
Gestation
E13.5
E14.5
E15.5
C
c-Maf +/-
c-Maf -/-
D
c-Maf +/+
47
0.69
27.2
15
c-Maf -/-
45.1
8.99
20.4
17.6
Cells
Propidium Iodide
Fraction (%)
Apotosis
G0-G1
S
G2-M

Figure 3

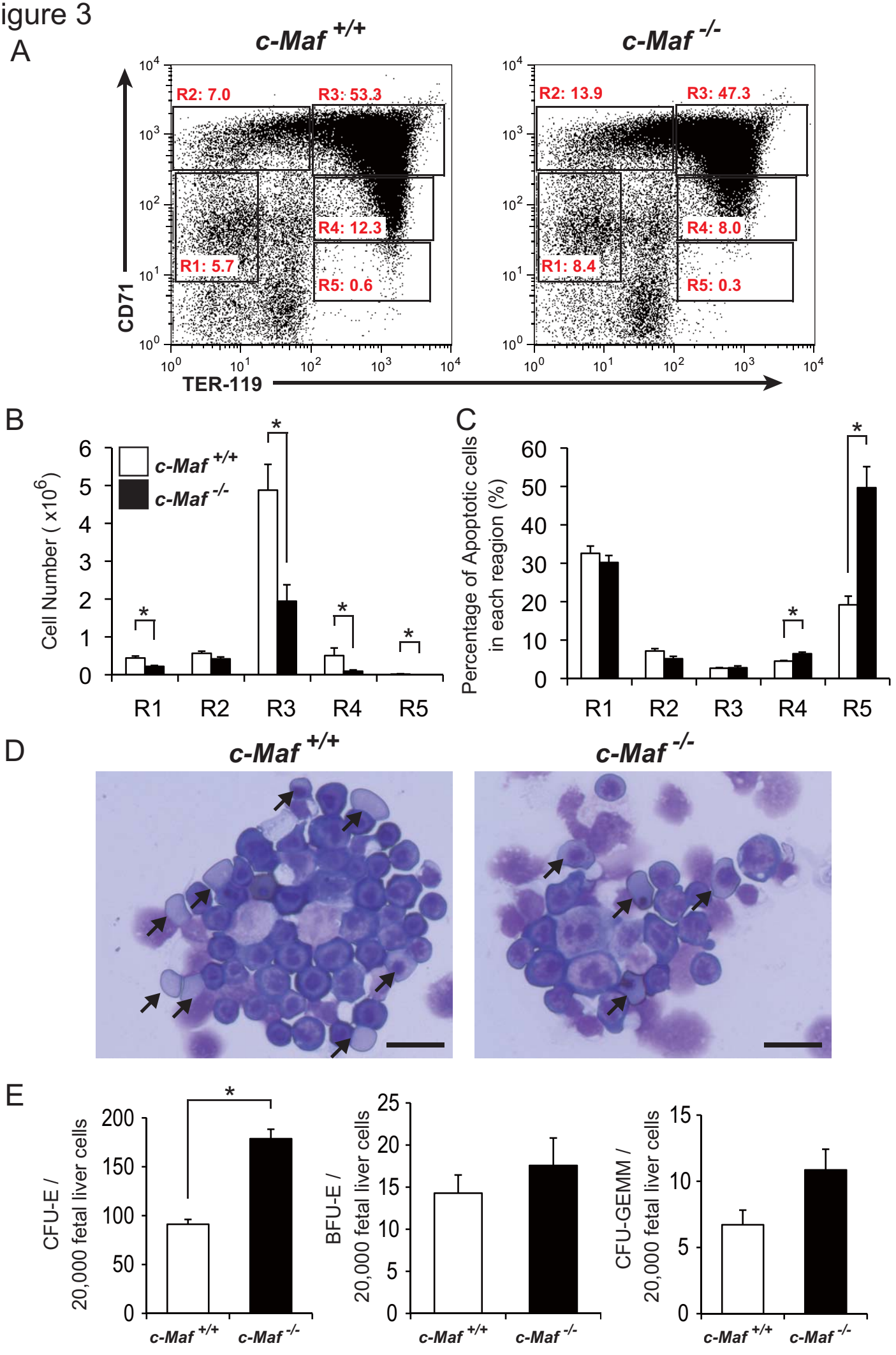
A
c-Maf +/+
c-Maf -/-
R2: 7.0
R3: 53.3
R4: 12.3
R1: 5.7
R5: 0.6
R2: 13.9
R3: 47.3
R4: 8.0
R1: 8.4
R5: 0.3
CD71
TER-119
B
Cell Number (x10^6)
c-Maf +/+
c-Maf -/-
R1
R2
R3
R4
R5
C
Percentage of Apoptotic cells in each reagion (%)
D
E
CFU-E / 20,000 fetal liver cells
BFU-E / 20,000 fetal liver cells
CFU-GEMM / 20,000 fetal liver cells

Figure 4

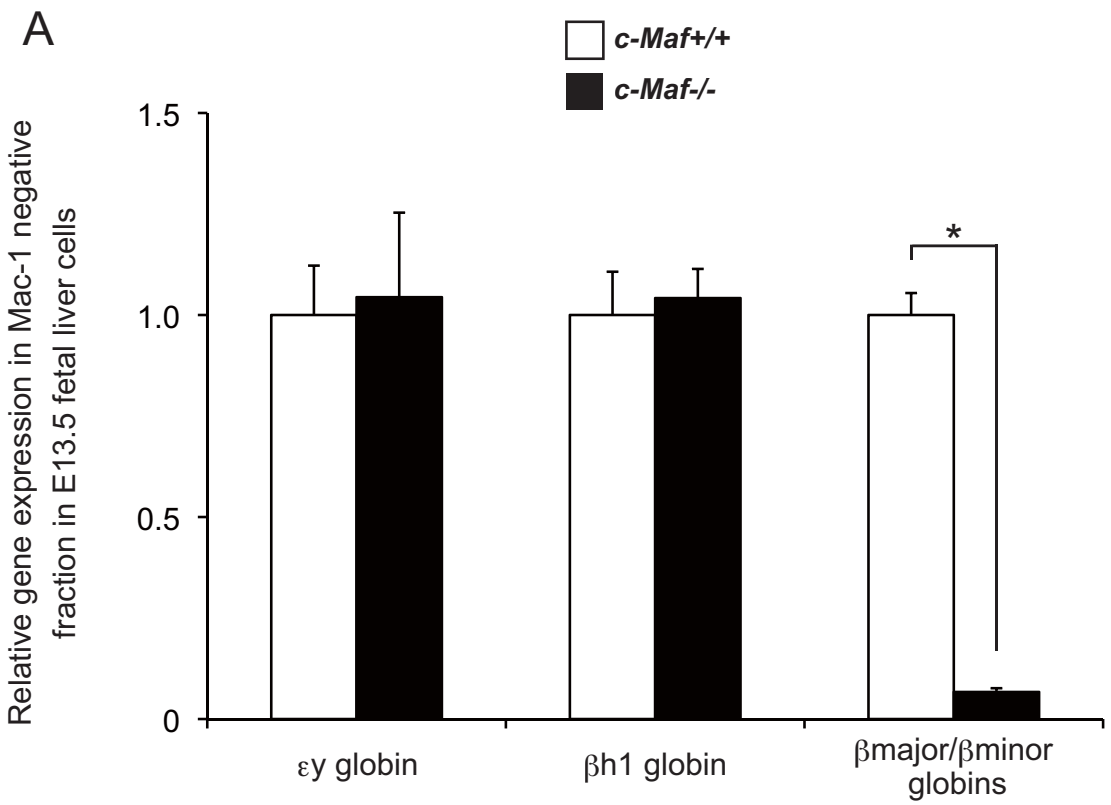
A
c-Maf+/+
c-Maf-/-
Relative gene expression in Mac-1 negative fraction in E13.5 fetal liver cells
1.5
1.0
0.5
0
*
εy globin
βh1 globin
βmajor/βminor globins

Figure 5

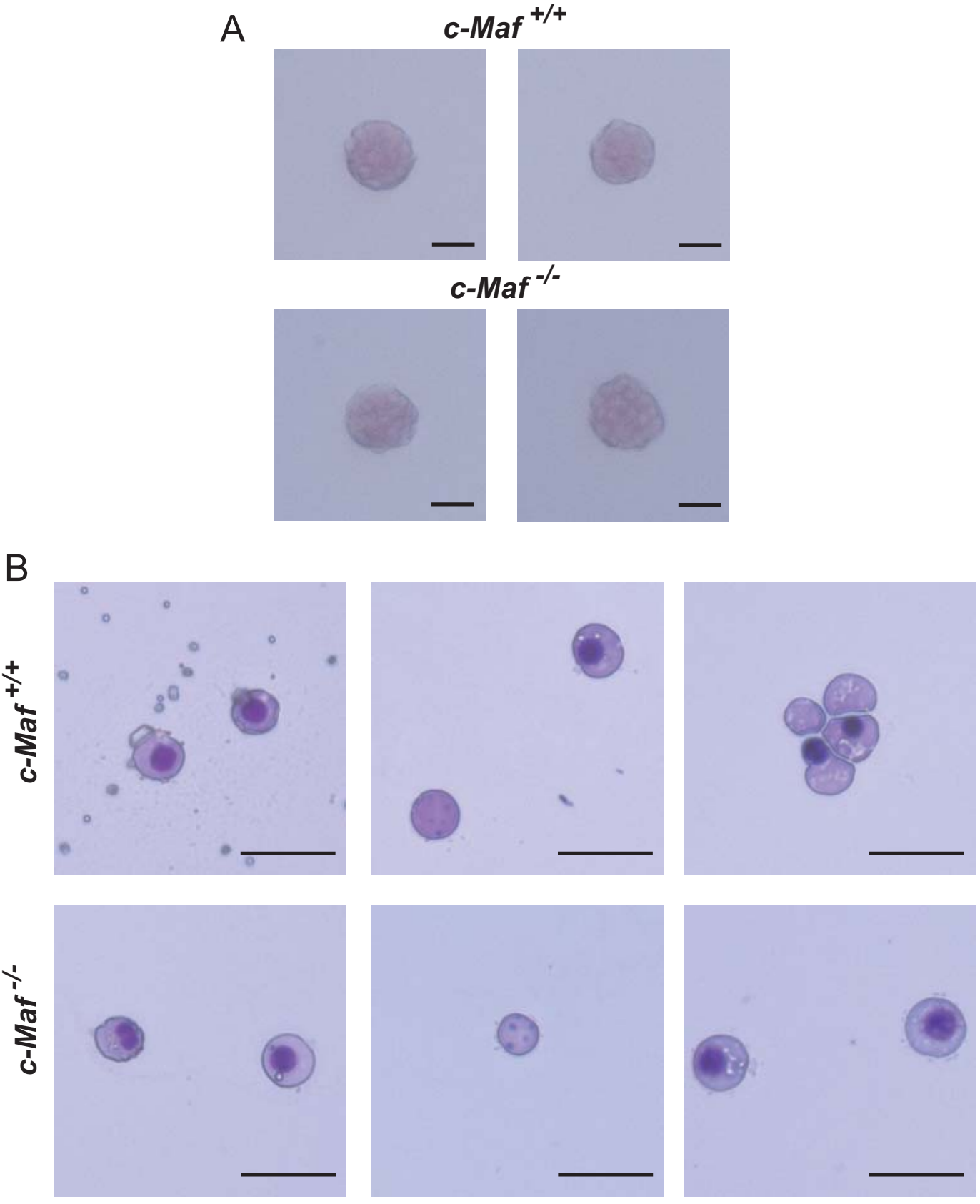

Figure 6

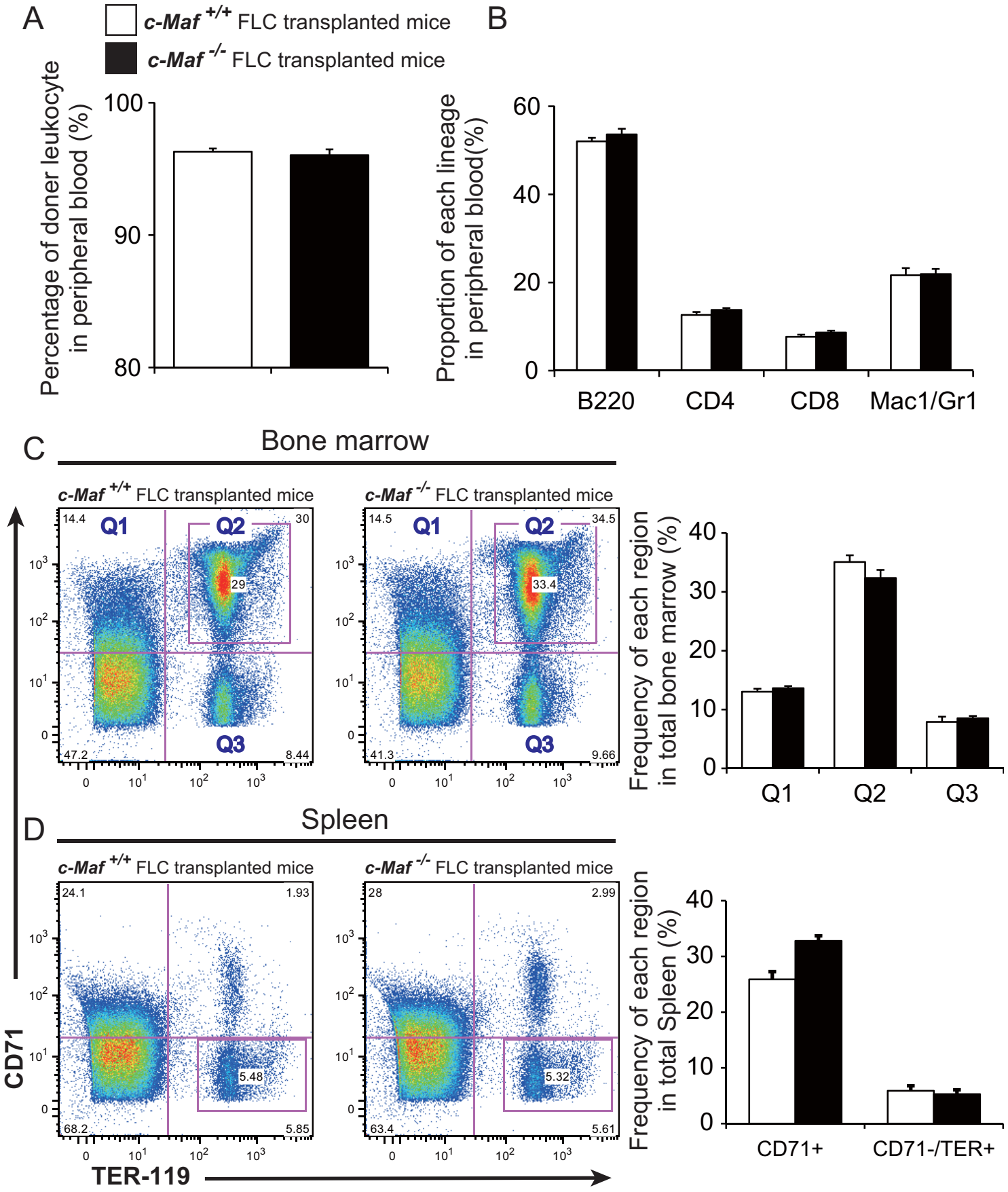
A
c-Maf +/+ FLC transplanted mice
c-Maf -/- FLC transplanted mice
Percentage of doner leukocyte in peripheral blood (%)
100
90
80
B
Proportion of each lineage in peripheral blood(%)
60
40
20
0
B220
CD4
CD8
Mac1/Gr1
C
Bone marrow
c-Maf +/+ FLC transplanted mice
c-Maf -/- FLC transplanted mice
Q1
Q2
Q3
14.4
30
29
47.2
8.44
14.5
34.5
33.4
41.3
9.66
Frequency of each region in total bone marrow (%)
40
30
20
10
0
Q1
Q2
Q3
D
Spleen
c-Maf +/+ FLC transplanted mice
c-Maf -/- FLC transplanted mice
24.1
1.93
5.48
68.2
5.85
28
2.99
5.32
63.4
5.61
CD71
TER-119
Frequency of each region in total Spleen (%)
40
30
20
10
0
CD71+
CD71-/TER+

Figure 7

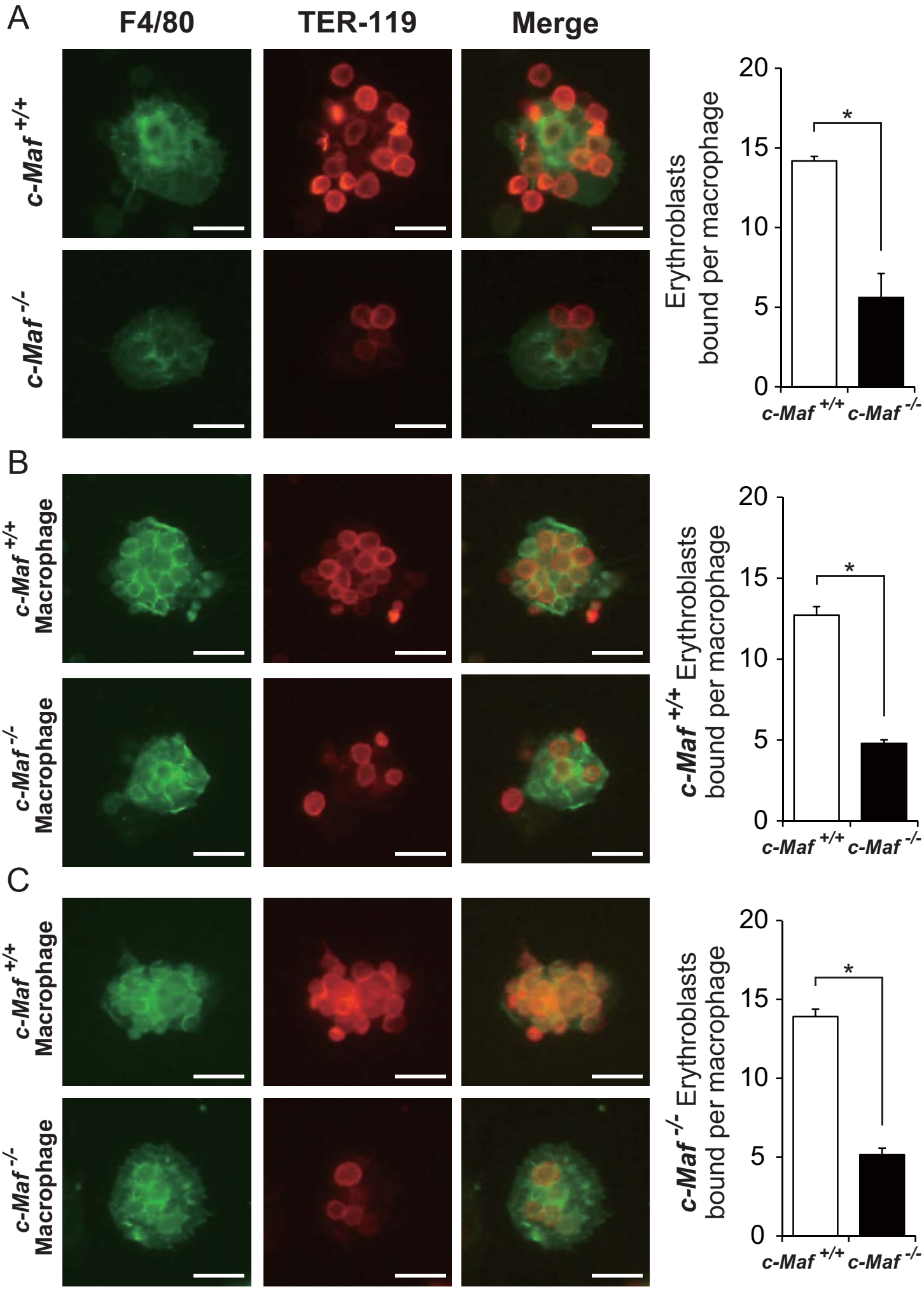
A
F4/80
TER-119
Merge
c-Maf +/+
c-Maf -/-
Erythroblasts bound per macrophage
20
15
10
5
0
*
c-Maf +/+
c-Maf -/-
B
c-Maf +/+ Macrophage
c-Maf -/- Macrophage
c-Maf +/+ Erythroblasts bound per macrophage
C
c-Maf +/+ Macrophage
c-Maf -/- Macrophage
c-Maf -/- Erythroblasts bound per macrophage

Figure 8

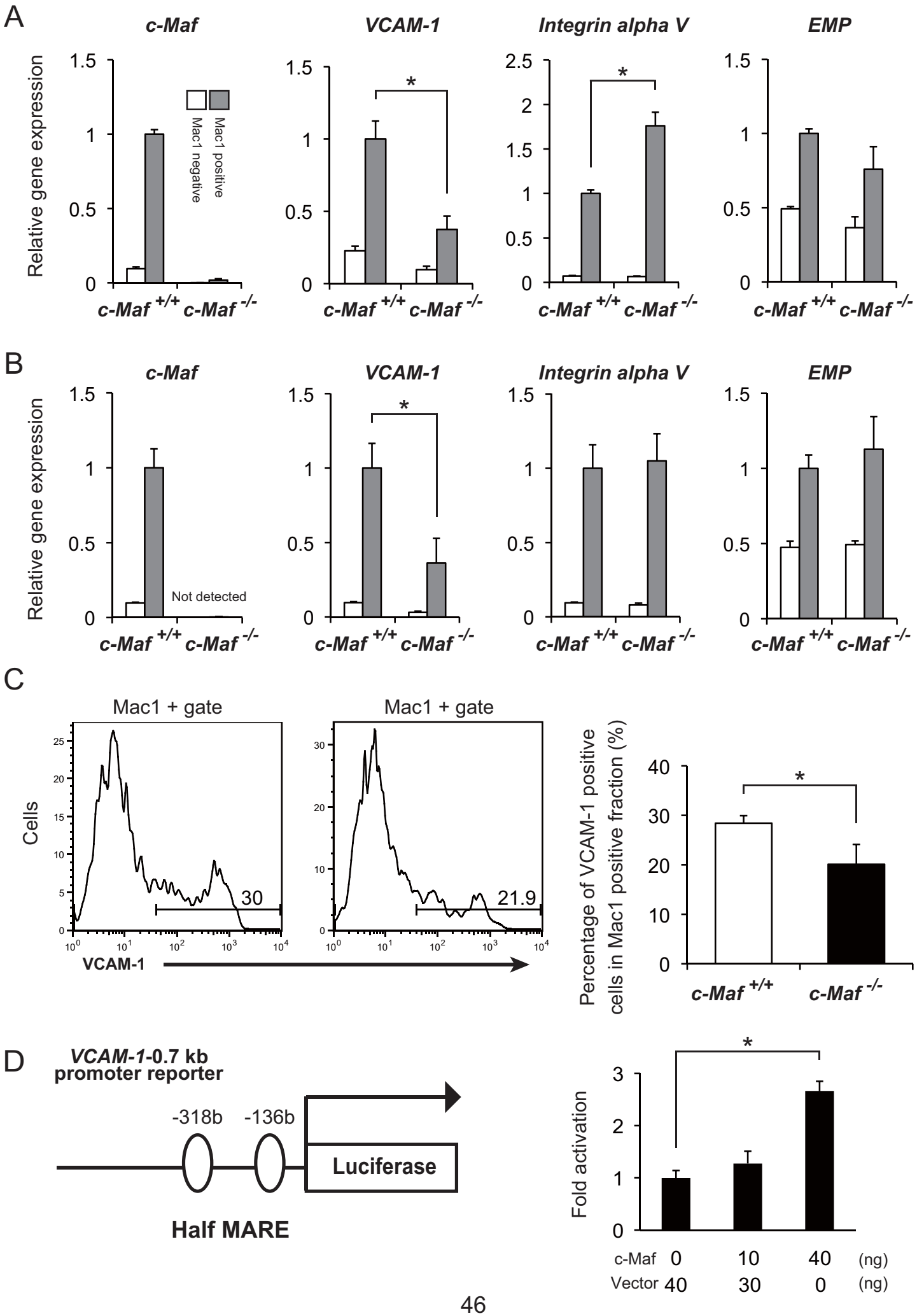
A
c-Maf
VCAM-1
Integrin alpha V
EMP
Relative gene expression
Mac1 negative
Mac1 positive
c-Maf +/+ c-Maf -/-
B
Not detected
C
Mac1 + gate
Cells
VCAM-1
30
21.9
Percentage of VCAM-1 positive cells in Mac1 positive fraction (%)
D
VCAM-1-0.7 kb promoter reporter
-318b
-136b
Luciferase
Half MARE
Fold activation
c-Maf 0 10 40 (ng)
Vector 40 30 0 (ng)

Figure 9

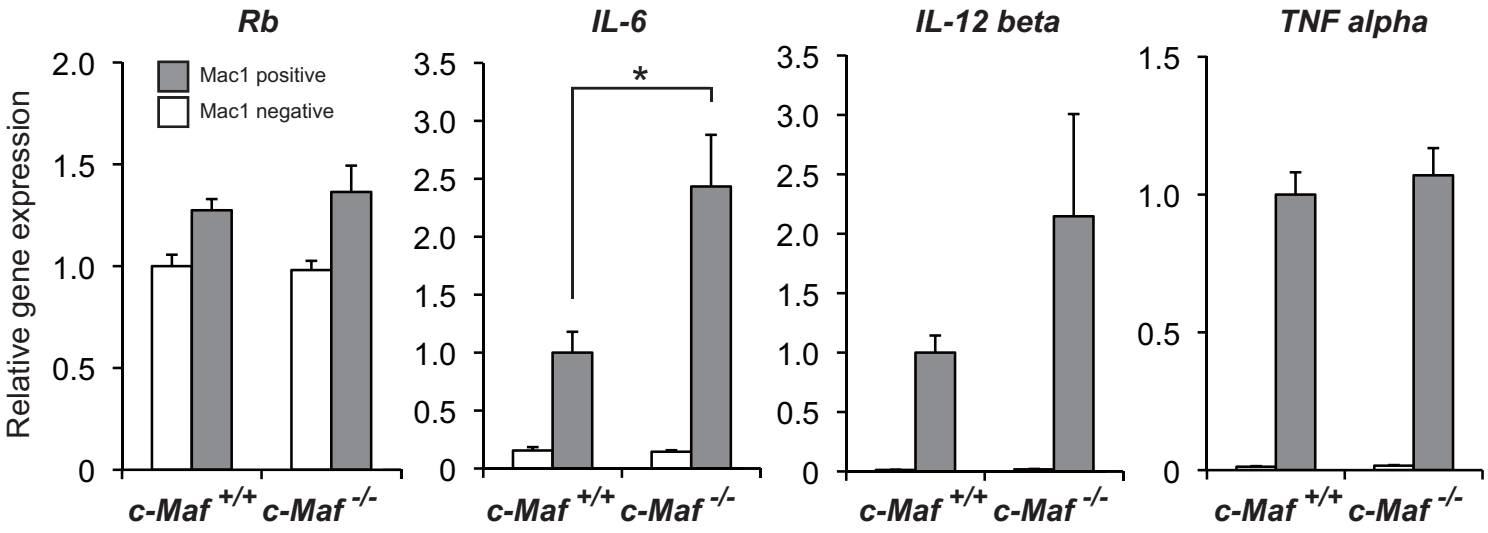
Rb
IL-6
IL-12 beta
TNF alpha
Relative gene expression
Mac1 positive
Mac1 negative
*
c-Maf +/+
c-Maf -/-